DOI: 10.1002/mds3.10132

RESEARCH ARTICLE

MEDICAL DEVICES & SENSORS WILEY

Biocompatible hydrogel ostomy adhesive

William Pan[1] | **Beverly Matsuda**[1] | **Hyunwoo Yuk**[2]

[1]Northwood High School, Irvine, CA, USA

[2]Department of Mechanical Engineering, Massachusetts Institute of Technology, Cambridge, MA, USA

Correspondence
William Pan, Northwood High School, Irvine, CA, USA.
Email: williampan4032@gmail.com

Hyunwoo Yuk, Department of Mechanical Engineering, Massachusetts Institute of Technology, Cambridge, MA, USA.
Email: hyunwoo@mit.edu

Abstract

Ostomies are digestive and excretory surgeries where waste is redirected to the outside of the abdomen, requiring a bag to catch excretion. Current methods use adhesives to create adhesion for 24-h usage of the ostomy bag. However, current adhesives are weak and unstable, and often lead to leakages of ostomy effluents resulting in various clinical complications including irritant dermatitis and infection. Due to these challenges, no commercially available product provides strong enough adhesion nor mechanical softness to prevent skin damage from ostomy leaks. In this work, we introduce a hydrogel ostomy adhesive (HOA) made from a tough double-network hydrogel based on polyacrylamide and sodium alginate that strongly adheres onto the skin for over 24 h and prevents leaks by maintaining fluid-tight sealing against regular bodily movements. The adhesion of HOA to abdominal skin is achieved by the topological adhesion formed by a biopolymer chitosan solution. The HOA's robust adhesion of an ostomy bag is demonstrated on *ex vivo* porcine skin and *in vivo* human skin and is compared with existing commercially available ostomy bag adhesives.

KEYWORDS
bandages, chitosan, contact dermatitis, hydrogel, ostomy, surgical stomas, tissue adhesive

1 | INTRODUCTION

With 700,000 affected annually (Grant et al., 2013), ostomies are life-saving redirective surgeries for those who have defective waste systems (e.g. urinary and digestive) caused by acute diverticulitis, colorectal cancer, trauma or inflammatory bowel disease (Burch, 2005; Dabirian et al., 2010). As a result of these surgical interventions, the stoma (i.e. an artificial opening) is created through the abdomen wall from the bladder, ileum or colon. To collect the stoma effluent, most use a one-piece closed ostomy bag that is often adhered around the stoma and disposed daily (Voergaard et al., 2007). Current ostomy bags have two main limitations that lead to leakage: (a) face plates that are ineffective interfaces due to their overly stiff composition and (b) weak adhesion resulting in short wear time and difficult application. While various commercially available adhesive pastes and glues have been introduced to reinforce adhesion of ostomy bag to abdominal skin, existing adhesives for ostomy bags still lack the ability to form strong and stable adhesion, often resulting in premature failures and leakages. Such leaked digestive effluent can damage surrounding skin tissues, creating painful swelling and dermatitis (Cressey et al., 2017; Pieper, 1996; Richbourg et al., 2007). Regrettably, as many as 34% of ostomy patients commonly develop chemical irritation of the skin as a result of leakages (Leong et al., 1994).

Commercially available ostomy bag faceplates are composed of two parts: the adhesive layer and a thin flexible polymeric film. The adhesive layer is a blend of polyisobutylene, pectin, gelatine and sodium carboxymethylcellulose, while the thin polymeric film is made from polyethylene. Owing to various problems from ostomy bags alone and its application to skin, ostomy patients commonly use a variety of methods for improved adhesion of ostomy bag and prevention of leakages. Diverse forms and materials of ostomy bag adhesives have been developed including adhesive pastes (Burch, 2011) and pectin-based powders (Boyles, 2010). In this work, three commonly used pastes and powders were used as comparisons. Karaya gum powder comes in the form of a dry slightly brown powder that is applied on both commercially available ostomy adhesive and skin and is composed of a polysaccharide exudate. Stomahesive

has a consistency of a thick brown hydrocolloid paste that acts as both an adhesive and a buffer from leaks, providing contour to irregularly shaped stomas. Ostobond is a white viscous solution of liquid latex, *N*-hexane and zinc oxide that is coated on the skin and adhesive (see Figure S2 for additional information and pictures of the adhesives).

However, these existing products show relatively weak adhesion strength with limited efficacy to prevent leakages from ostomy bags. Several strategies that utilize the injection of porcine or bovine collagen or synthetic hydrogels into the skin to create improved conformal adhesion of ostomy bags have been proposed (Arai & Okubo, 1999; Smith et al., 2007; Weidmann et al., 2014), but these methods still require complicated application procedures or surgery.

To address these challenges of close-fitting, stable, easy-to-apply sealed ostomy bags, this work introduces a hydrogel ostomy adhesive (HOA) capable of forming biocompatible, soft and durable adhesion and sealing of ostomy bags to skin that are uncomplicated to change. This work sought to achieve three specific aims: (a) to test mechanical softness, strength and biocompatibility of the HOA with the skin; (b) to test robust adhesion strength and toughness between the HOA and skin compared with the three commonly used pastes and powder adhesives mentioned above; and (c) to test endurance of the HOA attached to the skin. The HOA consists of a polyacrylamide–alginate tough hydrogel ring that allows for robust adhesion of ostomy bag to resist regular skin motions and weight from the bag. The HOA matches the mechanical properties of human tissues such as the skin to minimize tissue damage or discomfort from mismatch in mechanical properties (Yuk et al., 2019). The HOA forms robust yet stretchable adhesion to skin surface based on a chitosan tough adhesive that can form robust interfacial adhesion via diffusion of biopolymer chains and resultant topological adhesion (Li et al., 2017; Yang et al., 2018).

Hydrogels were chosen for the HOA because they have been shown to be safe in the medical field with highly favourable biocompatibility, tissue-like mechanical properties and high water content (Deligkaris et al., 2010; Grolman et al., 2019). While conventional hydrogels have been limited to weak mechanical strength (e.g. gelatine, agar), this work utilizes a recently developed hydrogel with high strength and fracture toughness (Sun et al., 2012). These recently developed hydrogels have enabled a broad range of new biomedical applications including drug-delivery wound dressings (Balakrishnan et al., 2005; Kokabi et al., 2007; Liang et al., 2019; Liu et al., 2018) and tissue adhesives (Li et al., 2017; Lih et al., 2012; Rahimnejad & Zhong, 2017; Ryu et al., 2011; Yang et al., 2018; Yuk, et al., 2019). In particular, this work takes advantage of recent advances in particular methods of robust wet adhesion of tough hydrogels (Li et al., 2017; Yang et al., 2018; Yuk, et al., 2019). The capability to establish robust adhesion on skin together with biocompatibility with human tissue, softness, high toughness and stretchability render tough hydrogels as an ideal candidate for ostomy adhesives. The adhesion performance of the HOA is characterized based on various standard mechanical testing methods in comparison with various commercially available ostomy bag adhesives. We further demonstrate the fluid-tight sealing of ostomy bags by the HOA under realistic loads and daily motion based on *ex vivo* porcine skin and *in vivo* human skin.

2 | RESULTS

2.1 | Design of the HOA and chitosan tissue adhesive

HOA placement on the ostomy is shown schematically in Figure 1. An 85-mm-outer diameter and a 25- to 35-mm-inner diameter ring has been laser cut from a 1-mm-thick tough hydrogel. The inner diameter size depends on the size of the ostomy. The HOA consists of the first polyacrylamide network crosslinked by a covalent crosslinker (*N*,*N*′-methylenebis(acrylamide)), and the second alginate network crosslinked by calcium ions to form a highly stretchable and tough double-network hydrogel (Sun et al., 2012).

To achieve durable adhesion of the HOA, two types of chitosan-based adhesives were designed based on previously reported methods (Li et al., 2017; Yang et al., 2018). The first chitosan tissue adhesive consists of a bridging polymer solution of chitosan with 2-(*N*-morpholino)ethanesulphonic acid (MES) buffer at pH 4.5 applied onto the abdomen (see Materials and Methods for further information on the preparation of the HOA and the adhesives). For stronger adhesion, an alternative second chitosan tissue adhesive EDC-NHS was prepared using first chitosan solution, 1-ethyl-3-(−3-dimethylaminopropyl) carbodiimide hydrochloride (EDC), and *N*-hydroxysuccinimide (NHS). Both chitosan adhesives are applied between the hydrogel and skin. Because chitosan dissolves in acidic solutions with pH below 6.5 (Yang et al., 2019), the higher pH of the hydrogel (around 7) allows pH-induced crosslinking of chitosan between the hydrogel and the skin. The chitosan provides strong and flexible topological adhesion between the HOA and the skin that can resist movement and mechanical wear. Furthermore, cationic characteristic of chitosan can provide antibiotic properties against bacteria, fungi and parasites, allowing for sanitation and protection from infection of the ostomy (Blacklow et al., 2019; Li & Mooney, 2016). Removal of the adhesive from the skin is done by applying a slightly acidic solution of MES buffer (pH 4.5) to the edge of bonding to dissolve the chitosan polymer network (Yang et al., 2018). Note that the weakly acidic MES buffer with pH 4.5 is regarded as not skin-sensitizing (Daniel et al., 2018).

2.2 | Mechanical properties of the HOA

The HOA has a Young's modulus of less than 10 kPa to match the moduli of skin (85 kPa) (McKee et al., 2011) in order to provide a flexible watertight seal. This mechanical softness of the HOA ensures conformal contact to the underlying skin surface compared with existing ostomy bag adhesives that are hard and inflexible.

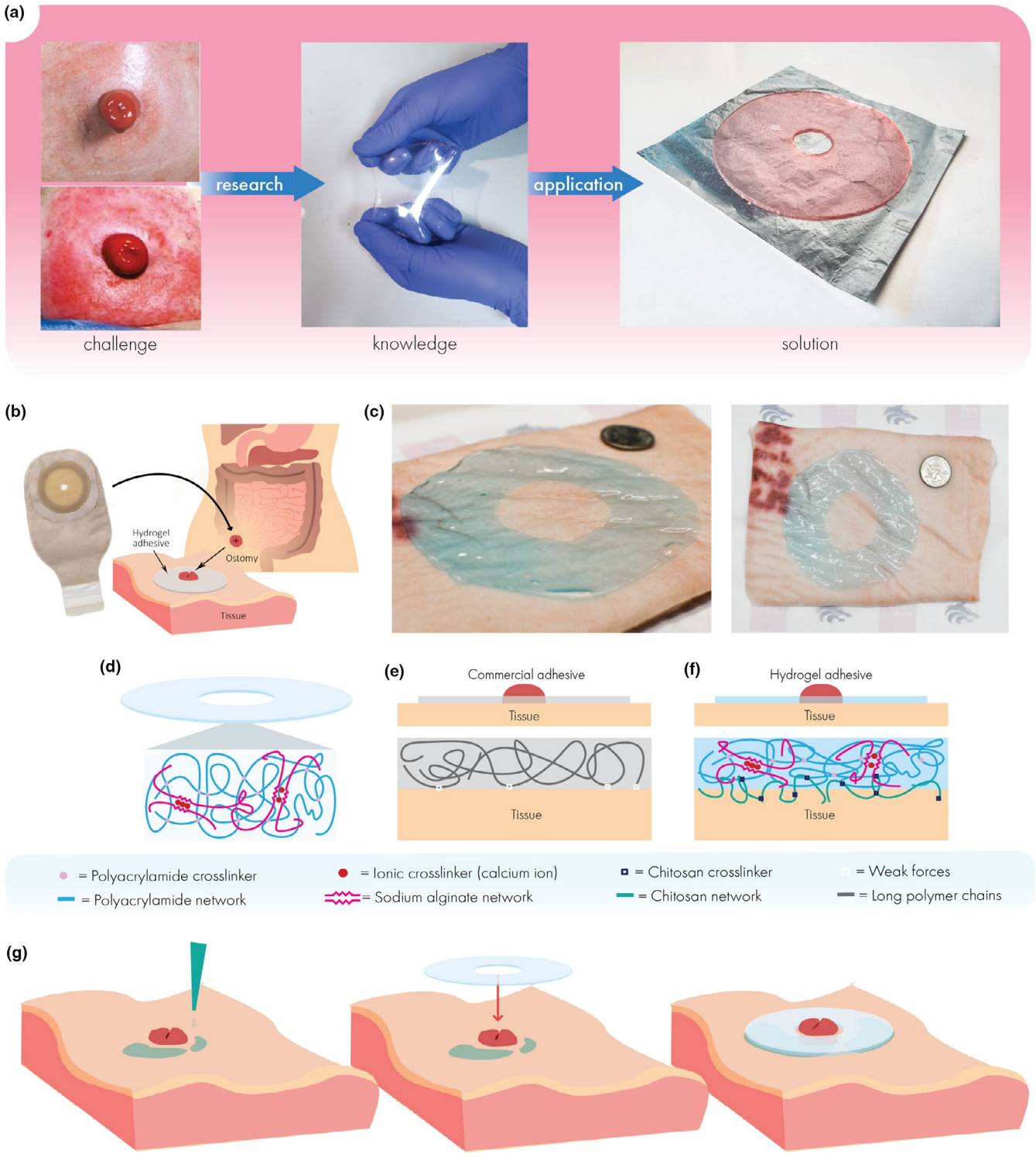

FIGURE 1 Design and mechanism of the HOA. (a) The top shows a normal stoma, while the bottom shows a stoma with dermatitis caused by leakages (Photo credit: ConvaTec). The HOA along with the chitosan tissue adhesive can provide improved adhesion of ostomy bag to skin. (b) The HOA is applied to the ascending colostomy. Devices, such as the ostomy bag as shown, can be applied to various other places such as transverse colostomy, jejunostomy and left colostomy. (c) Images of the HOA on porcine skin for in vitro testing. (d) The HOA consists of the double-network hydrogel of covalently crosslinked polyacrylamide and ionically crosslinked alginate networks. (e) Commercially available ostomy adhesives adhere to skin based on weak intermolecular forces such as van der Waal's forces to create temporary adhesion. (f) The HOA adheres to skin based on topological adhesion between the skin and the hydrogel network by chitosan polymers. (g) The application process of the HOA based on the chitosan adhesion solution

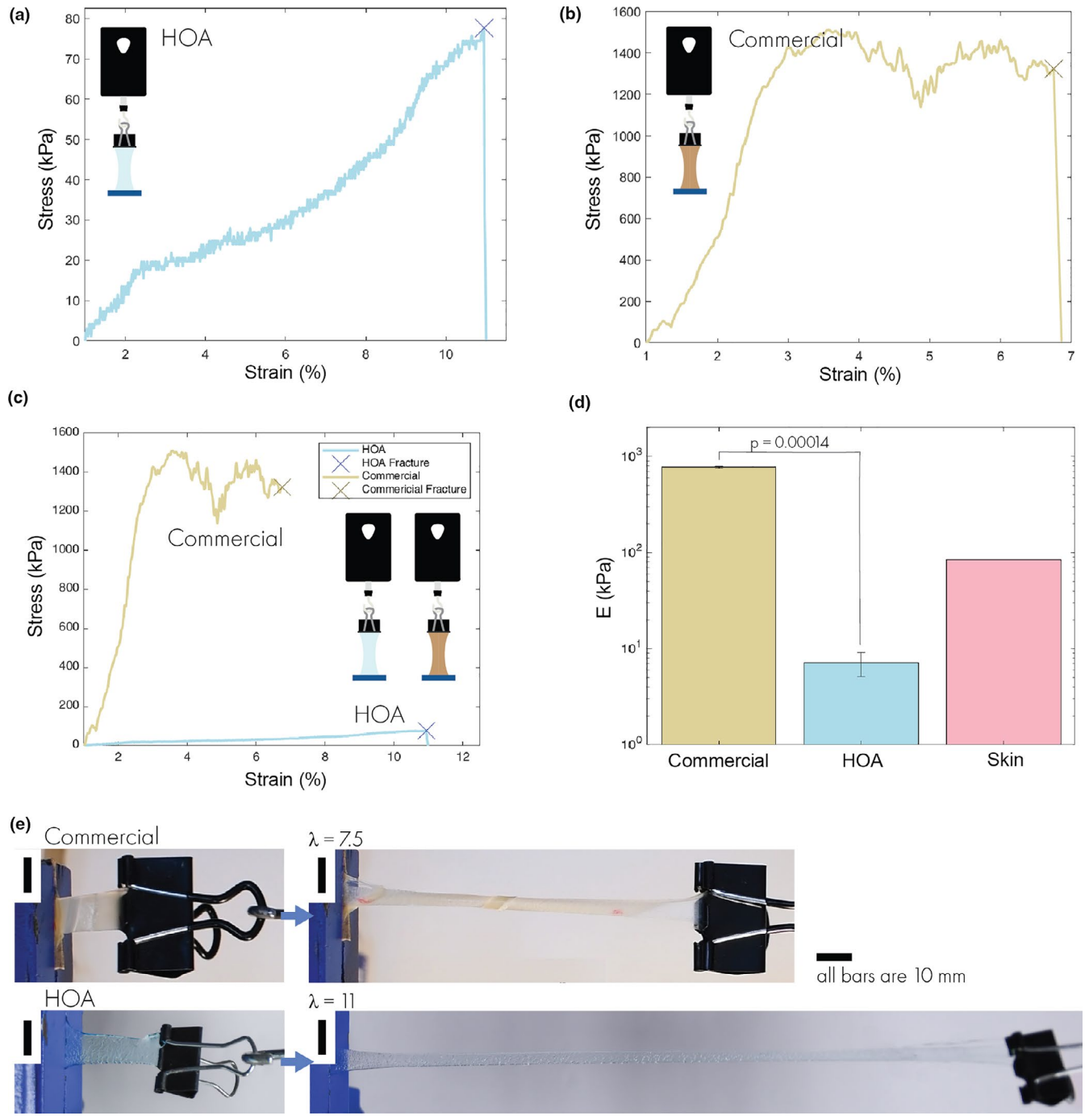

FIGURE 2 Mechanical properties of the HOA. (a) Engineering stress vs stretch curve of the HOA. (b) Engineering stress vs stretch curve of a commercially available ostomy bag material. (c) Engineering stress vs stretch curves of the HOA and the commercially available ostomy bag material shown together. (d) Young's modulus of the HOA, commercially available ostomy bag material and human skin. (e) Time-lapse images of the commercially available ostomy bag adhesives (top) and the HOA (bottom) near the maximum stretch. The bars represent a length of 10 mm. The *p*-value is calculated by the Student *t* test

Figure 2 shows that the HOA material can stretch up to 11 times its original length. The calculated Young's modulus (E) of the HOA is 7.12 ± 1.98 kPa. In contrast, commercially available ostomy bag face plates can only be stretched around 7.75 times before fracture, with the calculated Young's modulus of 772.45 ± 17.20 kPa (p = 0.00014).

2.3 | Adhesion and endurance performance of the HOA

An initial qualitative evaluation of HOA adhesion was done by applying the chitosan tissue adhesive solution on the HOA and human abdominal skin for 24 h (Figure 3(a)). While the HOA exhibits slight drying at the

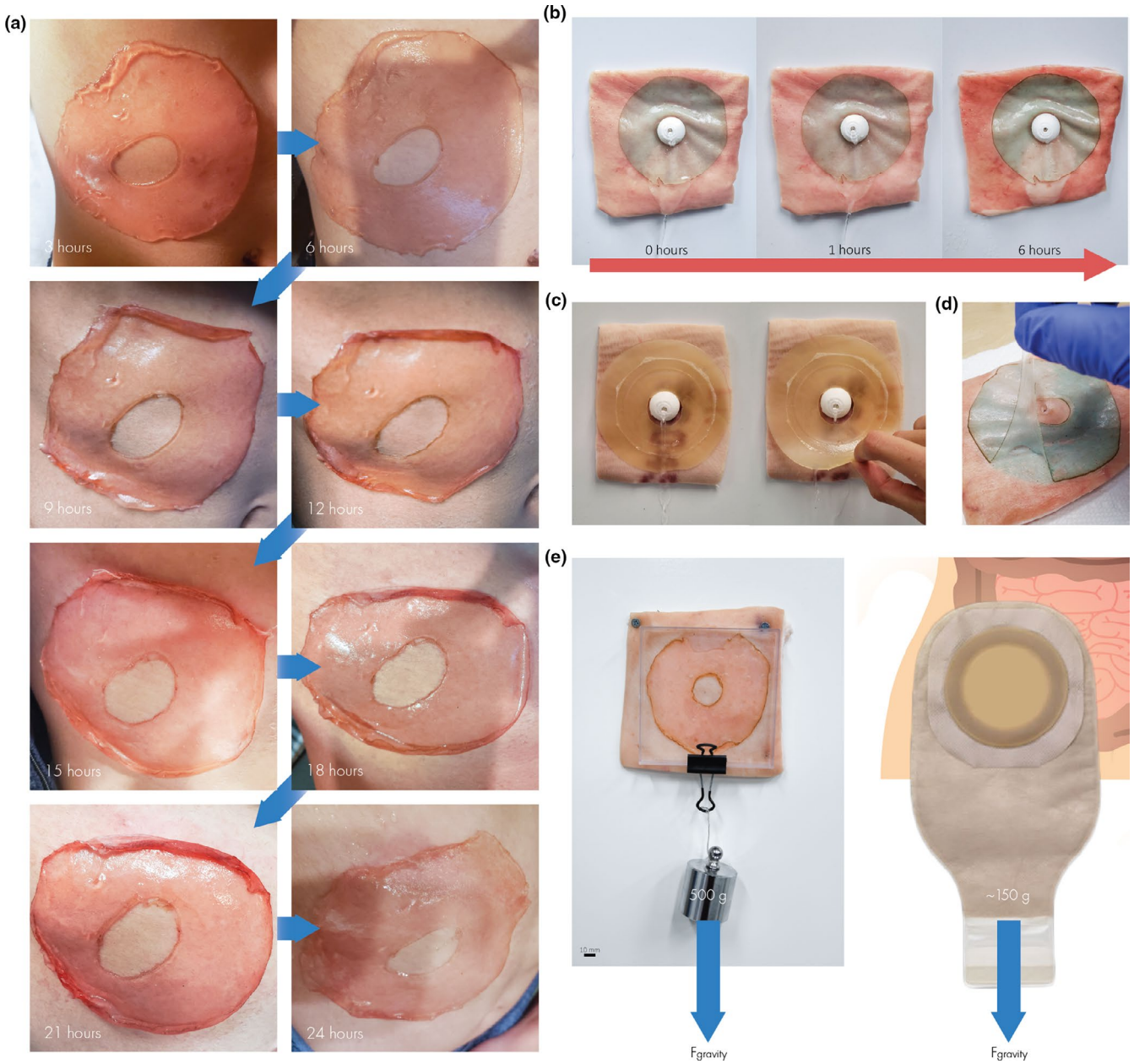

FIGURE 3 Robust and durable adhesion of the HOA on skin. (a) The HOA along with the chitosan tissue adhesive was applied onto the right hypochondriac and right lumbar of the abdomen skin. For every 3 hr, an image of the HOA was taken to monitor the adhesion and mechanical strength of the HOA. (b) Time-lapse photographs are shown of the HOA with adhered to chitosan tissue adhesive seconds after adhesion, 1 hr after adhesion, and 6 hr after adhesion on a mock ostomy tester based on porcine skin. (c) The durability test of commercially available ostomy bag adhesives shows weak bonding to the porcine skin when liquid flow was simulated. The adhesive can easily be peeled off and slip off the porcine skin. (d) Even after 12 hr of adhesion with the HOA, strong adhesion was present between the HOA and the porcine skin along with high mechanical strength. (e) The HOA was bonded to porcine skin for 12 hr and a plastic plate was adhered to the HOA to attach a 500 g weight (4.9 N of force)

outer edges over time, the majority of HOA retains robust adhesion to the skin. After one full day (i.e. 24 h), the HOA was still securely adhered to the abdomen. Longer adhesion times of over 24 h were considered while developing the HOA but were not performed at this time. Instead, it was opted to clean and replace the bag after 24 h to avoid the possibility of infection. Longer adhesion times could be explored in the future.

Quantitative results of the HOA's adhesion strength on *ex vivo* porcine skin (Figure 3(b)) shows the HOA ring provides sufficient adhesion strength to withstand forces up to 4.9 N (i.e. 500 g of weight) (Figure 3(e)). These results are above the average mass of typical ostomy bag capacity (~ 128 g) (Rose et al., 2015). After 6 h of testing on the mock ostomy set-up, the HOA retained its shape and strength (Figure 3(b)). Even after 12 h of adhesion to the porcine skin, the HOA still retains high stretchiness and strength (Figure 3(d)). In contrast, the commercially available ostomy bag adhesive shows weak adhesion and leakage (Figure 3(c)).

We further perform standard mechanical interfacial toughness and shear strength tests to compare the HOA with commercially available ostomy bag adhesives on porcine skin (Figure 4 and Figure S3). The commercially available adhesives show low interfacial toughness (37.5 J/m^2 for Karaya Powder; 15.3 J/m^2 for Ostobond; 12.6 J/m^2 for Stomahesive) and shear strength (4.28 kPa for Karaya Powder; 5.18 kPa for Ostobond; 4.40 kPa for Stomahesive). The HOA adhered by EDC-NHS chitosan adhesive shows much higher interfacial toughness (58.5 J/m^2) and shear strength (9.82 kPa).

3 | DISCUSSION

This work introduces a HOA as an alternative for ostomy patients as a promising solution to address the three previously proposed

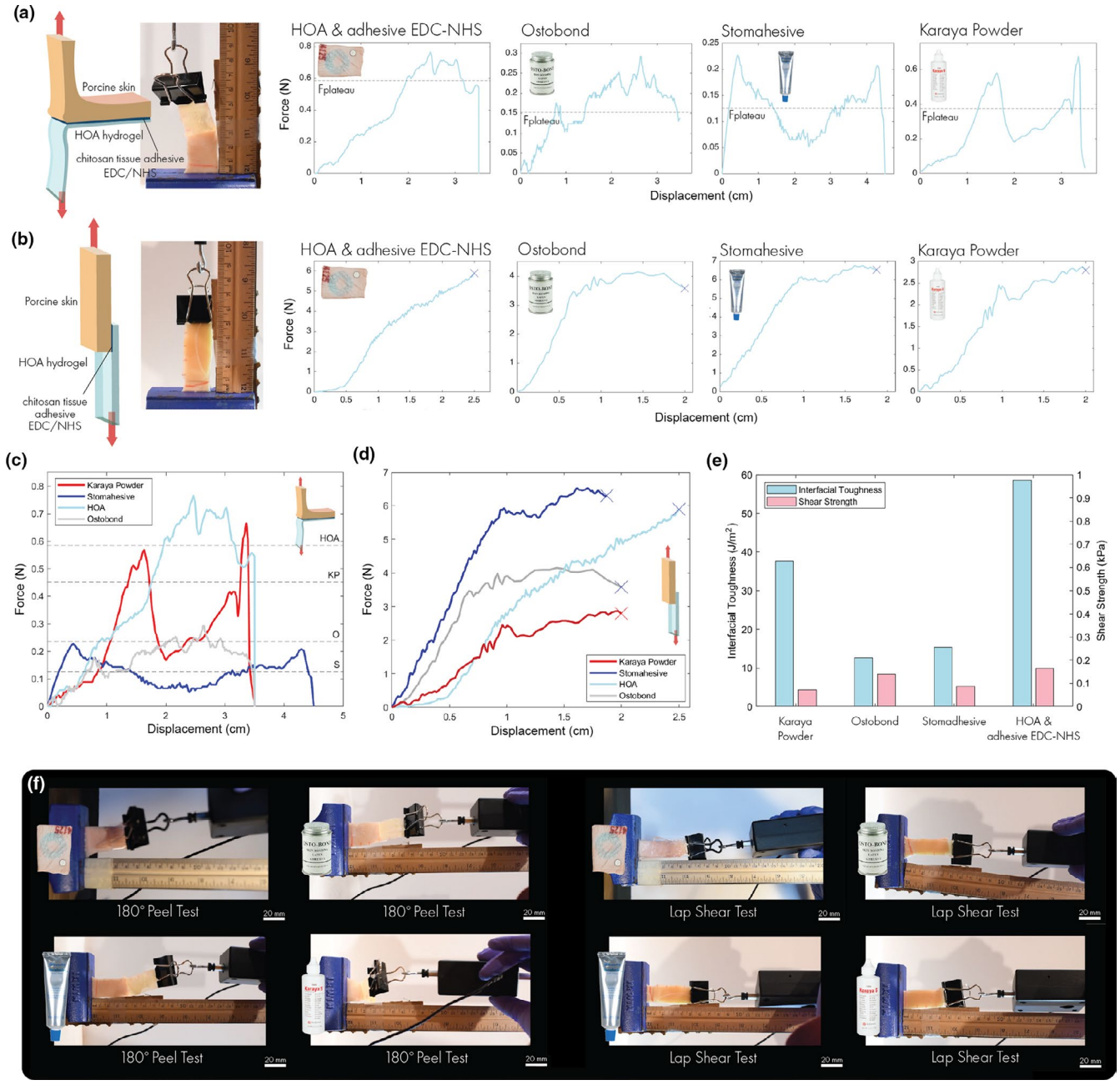

FIGURE 4 Adhesion performance of the HOA. (a) A 180° peel test was to determine the interfacial toughness of each of the different solutions. (Top left is Karaya Powder, top right is Stomahesive, bottom left is Ostobond, and bottom right is the HOA). (b) A lap shear test was used to determine the shear strength of each of the different solutions (Top left is Karaya Powder, top right is Stomahesive, bottom left is Ostobond, and bottom right is the HOA). (c) Representative testing curves for the 180° peel tests. (d) Representative testing curves for the lap shear tests. (e) Measured interfacial toughness and shear strength of the HOA and commercially available ostomy bag adhesives. (f) Representative images of the adhesion performance tests for the HOA and commercially available ostomy bag adhesives

aims not achieved by existing ostomy bag adhesives. Mechanical properties of the HOA is shown to be closer to that of the human skin through the comparison of Young's modulus, allowing for a soft, biocompatible and elastic interface that allows for ease of motion. Data from adhesion tests reveal that the HOA adhered with the chitosan tissue adhesive EDC/NHS had interfacial toughness and shear strength values that exceeded those of commercial pastes, powders and adhesives. A high shear strength from the tissue adhesive allows the HOA to stay adhered despite shear stress the ostomy bag applies on the adhesive. Strong adhesion can prevent the bag from coming loose during body movement. Lastly, through *in vivo* and *in vitro* testing of the HOA on human and porcine skin, the device showed remarkable endurance with wear times of up to 24 h, increasing the lifespan of ostomy bags and reducing the potential leakage of effluent onto the body. Combining these three properties, the HOA offers an interface closely resembling skin for flexibility and comfort and a soft, stretchable and durable adhesion between skin and ostomy bag that holds 0.5 kg of ostomy effluent over at least a 24-h duration to help prevent leakage of effluent. While this paper introduces a new product for consideration, clinical trials on various skin types while attaching an ostomy bag filled with liquid would need to be done before this product could ever be implemented. We present the introduction of the possibility of new materials.

The HOA could be improved by testing for longer duration times. Adding antidrying features on the hydrogel like a thin polydimethylsiloxane (PDMS) layer could prevent water from evaporating out of the hydrogel (Yuk et al., 2016) and thus increase viability of the material. On top of the HOA's capability as a robust adhesion agent for the ostomy bag in this work, the HOA has potential to be expanded with various other functionalities and methods. For example, drug delivery might be integrated into the surface of the HOA to administer medication such as hydrocortisone or other antihistamines that reduce inflammation after an accidental tear. A leak detection system might be another possible addition to the HOA where an alternating current could be passed through the gel, detecting bioimpedance changes to alert the patient of a potential leak. Furthermore, the HOA could potentially be modified to collect data on one's eating habits, by detecting and recording the various ions or vitamins from the patient's daily waste. We also envision that the robust integration of medical devices by the hydrogel adhesive demonstrated in this work may potentially be beneficial for other types of medical devices beyond ostomy bags.

4 | EXPERIMENTAL SECTION

4.1 | Materials

All reagents were obtained from Sigma-Aldrich unless noted otherwise and used without further purification. For the hydrogel monomers, acrylamide (AAm, A8887-100G, suitable for electrophoresis, 99%) and alginic acid sodium salt (sodium alginate, A1112-100G, low viscosity) were used. For the crosslinkers, *N*,*N*′-methylenebis(acrylamide) (MBAA, 146072-100G, 99%), *N*,*N*,*N*′,*N*′-tetramethylethylenediamine (TEMED, T22500-100ML, ReagentPlus®, 99%), ammonium persulphate (APS, A3678-25G, 98%) and calcium sulphate ($CaSO_4$, 255548-100G, 98%) were used as a covalent crosslinker, accelerator, initiator and ionic crosslinker, respectively.

Chitosan(448869-50G,lowmolecularweight)and2-(N-morpholino) ethanesulphonic acid (MES hydrate, M2933-25G) were used in formulating the chitosan tissue adhesive. The chitosan tissue adhesive EDC-NHS involved *N*-hydroxysuccinimide (NHS, 130672-5G, 98%) and *N*-(3-dimethylaminopropyl)-*N*′-ethylcarbodiimide hydrochloride (EDC, 03450-1G, 98%) as crosslinkers for the chitosan.

Glass panes and a silicone sheet (1.5 mm thick) were used as the mould for curing the hydrogel. Rain-X 2-in-1 Glass Cleaner +Rain Repellent was purchased at Target, which was used as a hydrophobic coating for the glass to decrease the adhesion of the hydrogel to the glass sheet. Hy-top® Assorted Food Coloring, which contained water, glycerine, FD&C Red #40, and FD&C Blue #1, was obtained at a local supermarket. Distilled water (dH_2O) was also obtained at a local supermarket.

Commercial ostomy adhesive solutions (Karaya Powder from ConvaTec®, Ostobond Skin Bonding Cement, and Convatec Stomahesive Paste) were obtained through Amazon and used as comparisons against the HOA. Current ostomy bags from Celecare were obtained from Amazon as well to facilitate mechanical test comparisons against the HOA.

For mechanical tests, a Dual-Range Force Sensor from Vernier measured the amount of force from shear, peel and tensile tests. A vice from Irwin secured porcine skin and adhesives. To record all tests and experiments, all photographs and videos were either taken on a Samsung S9 or a Nikon D500. Porcine belly skin was purchased at a local supermarket for in vitro testing of the hydrogel adhesive.

A mock simulation of ostomy-like conditions was created with plastic tubing and a plastic box bought from a local hardware store. A 3D printed mock stoma was designed in Fusion 360 and then printed with PLA in order to simulate a stoma in the mock test (images of the set-up are in Figure S4).

5 | METHODS

5.1 | Creation of the HOA Device

The creation of the hydrogel follows modified procedures from Sun et al. (2012) and Lin et al. (2016) (process of polymerization is in Figure S5). 1.028 g of sodium alginate and 5.3575 g of AAm were dissolved in 50 ml of dH_2O for 24 h until the sodium alginate was dissolved. About 10 μl of the blue or red food colouring was added in the solution for better visualization of the gel.

A glass mould was created by 2 glass panes 1 mm thick with a 1-mm-thick rubber sheet. The glass panes were lubricated by a hydrophobic coating to prevent the hydrogel from sticking to the glass

pane; in this case, Rain-X 2-in-1 Glass Cleaner +Rain Repellent was applied.

15 ml of the alginate/AAm solution was mixed with 600 μl of MBAA (0.2 g per 100 ml), 100 μl of APS (0.75 M), 400 μl of $CaSO_4$ (0.27 M) and 10 μl of TEMED. To prevent quick gelation of the alginate with the ionic crosslinker, the solution was quickly poured into the mould. Then, the gel was cured under UV light (365 nm) for 1 h. After curing was complete, the gel was submerged in dH_2O for 10 min to release some of the excess crosslinker and the hydrogel from the glass plate. Aluminium foil was then wrapped around the glass plate, and the hydrogel was then placed onto the aluminium foil to ease the cutting process. The gel was then vector cut to a predesigned shape in a laser cutter (Epilog Zing 24, 40 W) at 70% speed and 45% power, forming the HOA.

For the test requiring adhesion to in vivo human skin, the HOA was left to sit in dH_2O overnight and then was sprayed with isopropyl alcohol for further rinsing. Otherwise, the HOA was quickly stored in Ziploc® Freezer Quart Bags (images of assembling the HOA are included in Figure S6).

5.2 | Synthesis of the chitosan tissue adhesive

The tissue adhesive follows the same procedures from Li et al. (2017) and Yang et al. (2018); chitosan tissue adhesive EDC/NHS bonding mechanism is shown in Figure S7. 0.476 g of MES hydrate was dissolved into 50.0 ml of dH_2O. pH was not monitored to prevent cross-contamination with the pH probes, but approximate pH was around 4.5 to 6 pH. 0.5 g of chitosan was then dissolved into the MES hydrate solution for 1 h to completely mix. The solution was then covered and sat still for 24 h to release the remaining air bubbles in the solution. The solution is slightly viscous and has a light-yellow tinge.

The tissue adhesive EDC/NHS was made by creating a concentration of 12 mg/ml of NHS and EDC. In this case, 0.12 g of NHS was weighed and mixed in 5 ml of the chitosan/MES buffer solution as described previously. 0.12 g of EDC was mixed into another 5 ml of the chitosan/MES buffer solution to prevent NHS-EDC crosslinking before adhesive application. The solution was then covered and left to settle for 24 h. The solution is viscous but clearer than the solution described before.

To apply the adhesive solution, a micropipette was used to transfer the solution to the porcine skin. As a small droplet was applied onto the skin, the solution was then spread evenly to insure adhesion on all the adhesive (images of assembling the chitosan tissue adhesive are included in Figure S8).

5.3 | Mechanical tests on the HOA

Mechanical tests were used to compare the strength of the material of current ostomy adhesive backings with that of the HOA. Stress–strain curves of the device alongside the other current product were measured by stretching the material until rupture occurs. A 10 × 50 mm strip was cut from ostomy adhesives and the HOA. 10 mm of each side was anchored (one side with a vice and the other with a binder clip). A Dual-Range Force Sensor by Vernier or a mechanical tester (2.5 kN load-cell, Zwick/Roell Z2.5, Figure S3) was used for mechanical tests.

To compare the mechanical stiffness of the HOA, Young's modulus was used as the standard of comparison and was tested on porcine skin due to its similar mechanical properties and toughness like the human skin (Li et al., 2017). Young's modulus (E) is defined by the relation of stress by the amount of strain:

$$E = \frac{\sigma}{\epsilon} \tag{1}$$

$$E = \frac{F/A}{\Delta L/L_o} \tag{2}$$

To calculate Young's modulus for commercially available ostomy bags and the HOA, the tensile test data were plotted in engineering strain (i.e. displacement divided by the original gauze length) vs engineering stress (i.e. tensile force divided by the original cross-sectional area of the sample) and the linear slope at 2% engineering strain was taken as the Young's modulus.

5.4 | Adhesion tests of the tissue adhesive applied to the HOA

Current products on the market, such as Stomahesive, Ostobond and Karaya gum powder, were used as comparisons to the current device. Adhesion strength was determined through two tests. All tests were done on porcine skin. First, a lap shear test was used to determine shear strength. Shear strength was evaluated on each of the adhesives due to the ostomy bag's innate design, a bag with weight exerting a shear force on the adhesive to the skin.

20 mm × 50 mm strips of porcine skin and ostomy bag adhesive (from Celecare) were cut, and adhesives were then applied onto 40 mm of the strip, leaving 10 mm for anchoring purposes (a binder clip was clipped to the ostomy bag adhesive, while the vice secured the porcine skin). The Dual-Range Force Sensor was then hooked onto the binder clip and was pulled to create a shear motion (video recorded displacement of the porcine skin and ostomy bag adhesives; see Figure 4 for images of the set-up).

To derive shear strength, the maximum force is found until fracture and is divided by the total initial area of bonding:

$$\text{Shear Strength} = \frac{F_{max}}{WL} \tag{3}$$

where W is the width of the adhesive area, while L the length of the adhesive area.

Then, a peel test was used to test the resistance to peel forces. Methods were similar to that of the shear strength test. Adhesion

energy with peel tests was measured in terms of interfacial toughness with the units of kJ/m^2, while the shear test was measured in terms of shear with the units of kPa (see Figure 4 for images of the set-up).

Interfacial toughness can be defined as:

$$\Gamma = \Gamma_o + \Gamma_d \tag{4}$$

where Γ_o is equal to the chemically anchored interfacial toughness, Γ_d is equal to the interfacial toughness that is around the interface, and Γ is equal to the total interfacial toughness of adhesion. $F_{plateau}$ is found by determining the steady state of the peel test. The peeling rate of 50 mm/min was used to measure interfacial toughness (Figure S3). A simple calculation can then be done to find Γ through the equation after measuring the force plateau of the peel test:

$$\Gamma = \frac{F_{plateau}}{2W} \tag{5}$$

Additionally, as a qualitative measure of adhesion strength, the HOA was attached to porcine skin with the chitosan tissue adhesive and an 11 cm × 11 cm plastic plate or ostomy bags were attached to the HOA by cyanoacrylate glue (Loctite Super Glue). Once the plate was attached while in contact with the HOA, a 500 g mass was clipped onto the ledge of the plastic plate and was suspended for 20–30 min.

5.5 | Device endurance tests

The endurance of the device was first measured in vitro. A mock set-up simulated the environment of an ostomy. A tube was attached to a supply of tap water. The other end of the tube led to a 3D printed stoma that allowed for water leakage to simulate the process of excretion (images of the set-up are included in Figure S4). Over the course of 12 h, the HOA was left out adhered on porcine skin attached to the mock set-up. A light stream of water was continuously run through the mockup and onto the HOA device. Every hour, an image was recorded to determine the endurance of the device in terms of hydration and drug delivery.

For the in vivo test, the HOA device was adhered onto the forearm or the right hypochondriac and right lumbar of the abdomen for 24 h. The human patient participated in the experiment with consent (the author, W.P.), and the safety precautions were taken to ensure the experiment caused no pain, irritation or damage to the human patient's skin based on the Material Safety Data Sheets (MSDS) of the HOA and chitosan adhesive. An image was then taken every 3 hr to record the status of the device.

ACKNOWLEDGEMENTS

The authors thank Leslie Fuchs M.D. (University of California Berkeley), Claire Thomas Ph.D. (University of California Berkeley), Prabudhya Bhattacharyya (University of California Berkeley) and Marcus Chao (Rhode Island School of Design) for developing the idea of a hydrogel adhesive at MIT Grand Hack San Francisco 2019; and David Monge (Northwood High School), Matt Marshall (Northwood High School), Nicole Midani (Northwood High School) and Kyle Kim-E (Northwood High School) for supervising experiments and development of the device.

REFERENCES

Arai, Y., & Okubo, K. (1999). Correction of dermal contour defect with collagen injection: A simple management technique for difficult stomal care. *The Journal of Urology*, *161*(2), 601-602.

Balakrishnan, B., Mohanty, M., Umashankar, P., & Jayakrishnan, A. (2005). Evaluation of an in situ forming hydrogel wound dressing based on oxidized alginate and gelatin. *Biomaterials*, *26*(32), 6335–6342. https://doi.org/10.1016/j.biomaterials.2005.04.012

Blacklow, S. O., Li, J., Freedman, B. R., Zeidi, M., Chen, C., & Mooney, D. J. (2019). Bioinspired mechanically active adhesive dressings to accelerate wound closure. *Science Advances*, *5*(7), eaaw3963. https://doi.org/10.1126/sciadv.aaw3963

Boyles, A. (2010). Keeping up to date with stoma care accessories: Enabling informed choice. *Gastrointestinal Nursing*, *8*(6), 24–38. https://doi.org/10.12968/gasn.2010.8.6.49020

Burch, J. (2005). Exploring the conditions leading to stoma-forming surgery. *British Journal of Nursing*, *14*(2), 94–98. https://doi.org/10.12968/bjon.2005.14.2.17438

Burch, J. (2011). Stoma care-related skin problems and solutions. *British Journal of Nursing*, *20*(21), 1358.

Cressey, B. D., Belum, V. R., Scheinman, P., Silvestri, D., McEntee, N., Livingston, V., Lacouture, M. E., & Zippin, J. H. (2017). Stoma care products represent a common and previously underreported source of peristomal contact dermatitis. *Contact Dermatitis*, *76*(1), 27–33. https://doi.org/10.1111/cod.12678

Dabirian, A., Yaghmaei, F., Rassouli, M., & Tafreshi, M. Z. (2010). Quality of life in ostomy patients: A qualitative study. *Patient Preference and Adherence*, *5*, 1–5. https://doi.org/10.2147/PPA.S14508

Daniel, A. B., Strickland, J., Allen, D., Casati, S., Zuang, V., Barroso, J., Whelan, M., Régimbald-Krnel, M. J., Kojima, H., Nishikawa, A., Park, H.-K., Lee, J. K., Kim, T. S., Delgado, I., Rios, L., Yang, Y., Wang, G., & Kleinstreuer, N. (2018). International regulatory requirements for skin sensitization testing. *Regulatory Toxicology and Pharmacology*, *95*, 52–65. https://doi.org/10.1016/j.yrtph.2018.03.003

Deligkaris, K., Tadele, T. S., Olthuis, W., & van den Berg, A. (2010). Hydrogel-based devices for biomedical applications. *Sensors and Actuators B: Chemical*, *147*(2), 765–774. https://doi.org/10.1016/j.snb.2010.03.083

Grant, M., McCorkle, R., Hornbrook, M. C., Wendel, C. S., & Krouse, R. (2013). Development of a chronic care ostomy self-management program. *Journal of Cancer Education*, *28*(1), 70-78. https://doi.org/10.1007/s13187-012-0433-1

Grolman, J. M., Singh, M., Mooney, D. J., Eriksson, E., & Nuutila, K. (2019). Antibiotic-containing agarose hydrogel for wound and burn care. *Journal of Burn Care & Research*, *40*(6), 900–906. https://doi.org/10.1093/jbcr/irz113

Kokabi, M., Sirousazar, M., & Hassan, Z. M. (2007). PVA–clay nanocomposite hydrogels for wound dressing. *European Polymer Journal*, *43*(3), 773-781. https://doi.org/10.1016/j.eurpolymj.2006.11.030

Leong, A. P. K., Londono-Schimmer, E. E., & Phillips, R. K. S. (1994). Life-table analysis of stomal complications following ileostomy. *British Journal of Surgery*, *81*(5), 727-729. https://doi.org/10.1002/bjs.1800810536

Li, J., Celiz, A. D., Yang, J., Yang, Q., Wamala, I., Whyte, W., Seo, B. R., Vasilyev, N. V., Vlassak, J. J., Suo, Z., & Mooney, D. J. (2017). Tough adhesives for diverse wet surfaces. *Science*, *357*(6349), 378–381. https://doi.org/10.1126/science.aah6362

Li, J., & Mooney, D. J. (2016). Designing hydrogels for controlled drug delivery. *Nature Reviews. Materials*, *1*(12), https://doi.org/10.1038/natrevmats.2016.71

Liang, Y., Zhao, X., Hu, T., Han, Y., & Guo, B. (2019). Mussel-inspired, antibacterial, conductive, antioxidant, injectable composite hydrogel wound dressing to promote the regeneration of infected skin. *Journal of Colloid and Interface Science*, *556*, 514-528. https://doi.org/10.1016/j.jcis.2019.08.083

Lih, E., Lee, J. S., Park, K. M., & Park, K. D. (2012). Rapidly curable chitosan–PEG hydrogels as tissue adhesives for hemostasis and wound healing. *Acta Biomaterialia*, *8*(9), 3261–3269. https://doi.org/10.1016/j.actbio.2012.05.001

Lin, S., Yuk, H., Zhang, T., Parada, G. A., Koo, H., Yu, C., & Zhao, X. (2016). Stretchable Hydrogel Electronics and Devices. *Advanced Materials*, *28*(22), 4497–4505. https://doi.org/10.1002/adma.20150415

Liu, Q., Nian, G., Yang, C., Qu, S., & Suo, Z. (2018). Bonding dissimilar polymer networks in various manufacturing processes. *Nature Communications*, *9*(1), 846. https://doi.org/10.1038/s41467-018-03269-x

McKee, C. T., Last, J. A., Russell, P., & Murphy, C. J. (2011). Indentation versus tensile measurements of Young's modulus for soft biological tissues. *Tissue Engineering. Part B, Reviews*, *17*(3), 155–164. https://doi.org/10.1089/ten.TEB.2010.0520

Pieper, B. (1996). Predischarge and postdischarge concerns of persons with an ostomy*1. *Journal of WOCN*, *23*(2), 105–109. https://doi.org/10.1016/S1071-5754(96)90070-4

Rahimnejad, M., & Zhong, W. (2017). Mussel-inspired hydrogel tissue adhesives for wound closure. *RSC Advances*, *7*(75), 47380–47396. https://doi.org/10.1039/C7RA06743G

Richbourg, L., Thorpe, J. M., & Rapp, C. G. (2007). Difficulties experienced by the ostomate after hospital discharge. *Journal of Wound, Ostomy and Continence Nursing*, *34*(1), 70–79. https://doi.org/10.1097/00152192-200701000-00011

Rose, C., Parker, A., Jefferson, B., & Cartmell, E. (2015). The characterization of feces and urine: A review of the literature to inform advanced treatment technology. *Critical Reviews in Environmental Science and Technology*, *45*(17), 1827–1879. https://doi.org/10.1080/10643389.2014.1000761

Ryu, J. H., Lee, Y., Kong, W. H., Kim, T. G., Park, T. G., & Lee, H. (2011). Catechol-functionalized chitosan/pluronic hydrogels for tissue adhesives and hemostatic materials. *Biomacromolecules*, *12*(7), 2653–2659. https://doi.org/10.1021/bm200464x

Smith, G. H. M., Skipworth, R. J. E., Terrace, J. D., Helal, B., Stewart, K. J., & Anderson, D. N. (2007). Paraileostomy recontouring by collagen sealant injection: A novel approach to one aspect of ileostomy morbidity. Report of a case. *Diseases of the Colon & Rectum*, *50*(10), 1719–1723. https://doi.org/10.1007/s10350-007-9052-z

Sun, J.-Y., Zhao, X., Illeperuma, W. R. K., Chaudhuri, O., Oh, K. H., Mooney, D. J., Vlassak, J. J., & Suo, Z. (2012). Highly stretchable and tough hydrogels. *Nature*, *489*(7414), 133–136. https://doi.org/10.1038/nature11409

Voergaard, L. L., Vendelbo, G., Carlsen, B., Jacobsen, L., Nissen, B., Mortensen, J., Hansen, G., Bach, K., & Bæch, S. B. (2007). Ostomy bag management: Comparative study of a new one-piece closed bag. *British Journal of Nursing*, *16*(2), 95-–101. 10.12968/bjon.2007.16.2.22767

Weidmann, A. K., Al-Niaimi, F., & Lyon, C. C. (2014). Correction of skin contour defects in leaking stomas by filler injection: A novel approach for a difficult clinical problem. *Dermatology and Therapy*, *4*(2), 271–279. https://doi.org/10.1007/s13555-014-0058-x

Yang, J., Bai, R., Chen, B., & Suo, Z. (2019). Hydrogel adhesion: A supramolecular synergy of chemistry, topology, and mechanics. *Advanced Functional Materials*, *30*(2), 1901693. https://doi.org/10.1002/adfm.201901693

Yang, J., Bai, R., & Suo, Z. (2018). Topological adhesion of wet materials. *Advanced Materials*, *30*(25), 1800671. https://doi.org/10.1002/adma.201800671

Yuk, H., Lu, B., & Zhao, X. (2019). Hydrogel bioelectronics. *Chemical Society Reviews*, *48*(6), 1642–1667. https://doi.org/10.1039/C8CS00595H

Yuk, H., Varela, C. E., Nabzdyk, C. S., Mao, X., Padera, R. F., Roche, E. T., & Zhao, X. (2019). Dry double-sided tape for adhesion of wet tissues and devices. *Nature*, 1–6. https://doi.org/10.1038/s41586-019-1710-5

Yuk, H., Zhang, T., Parada, G. A., Liu, X., & Zhao, X. (2016). Skin-inspired hydrogel–elastomer hybrids with robust interfaces and functional microstructures. *Nature Communications*, *7*(1), 12028. https://doi.org/10.1038/ncomms12028

SUPPORTING INFORMATION

Additional supporting information may be found online in the Supporting Information section.

How to cite this article: Pan W, Matsuda B, Yuk H. Biocompatible hydrogel ostomy adhesive. *Med Devices Sens*. 2020;00:e10132. https://doi.org/10.1002/mds3.10132

Supplementary Information for

Biocompatible Ostomy Bag Hydrogel Adhesive

William Pan[a*], Beverly Matsuda[a], Hyunwoo Yuk[b*]

[1]Northwood High School, 4515 Portola Pkwy, Irvine, CA 92620, United States; [2]Department of Mechanical Engineering, Massachusetts Institute of Technology, Cambridge, MA 02139

*Correspondence and requests for materials should be addressed to W.P. (williampan4032@gmail.com) and H.Y. (hyunwoo@mit.edu)

This PDF file includes:

Supplementary Texts
Supplementary Figures 1 to 8
Supplementary References

Other Supplementary Materials for this manuscript include the following:

Supplementary Videos 1 to 7

Supplementary Note 1 – Quantitative Model for the HOA.

Ogden Model. As used by Zhang et al. 2017, to model elastic properties of the HOA, the Ogden model is used:

$$U_{ela} = \frac{2\mu}{\alpha^2}(\lambda_1^\alpha + \lambda_2^\alpha + \lambda_3^\alpha - 3) \quad \text{(Eq. 1)}$$

$$U = \eta U_{ela} + \Phi(\eta) \quad \text{(Eq. 2)}$$

$$\Phi(\eta) = \int_1^\eta \left[(m_\beta U_{dev}^{mp}) erf^{-1}(r(1-\eta)) U_{dev}^{mp}\right] d\eta \quad \text{(Eq. 3)}$$

where U_{ela} is the strain energy density, μ represents the initial moduli, of the gel, and α represents the Ogden parameter. λ represents the i^{th} principal stretch.

Mullin's effect. In order to model the stress and strain of elastomers under cyclic loadings, Mullins effect must be considered.

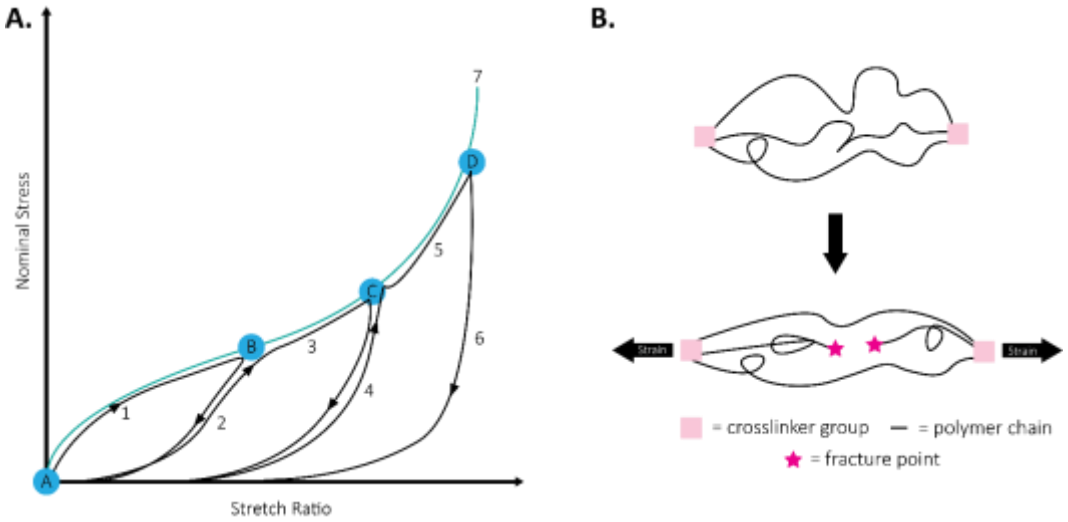

Supplementary Figure 1 | Mullin's effect. a. The primary loading path of an unstressed elastomer is shown through the teal line. As the elastomer is stressed for the first time, the stress follows the primary loading path to point B, but once unloaded, it follows line 2 as the molecular matrix of the gel is weakened. The first loading path (the one that is unsoftened) is known as the primary hyper elastic behavior. If cyclic loading occurs from point A to point B, it will continue to follow line 2. If stressed even more to point C, the unloading will lead follow line 4, retracing back to the weaker path. **b.** The intermolecular damage occurs in the polymer chain when stress is applied to the material, causing softening in the material to be unrecoverable.

A strain energy potential function $U(\mathbf{F})$ defines the strain energy and can be defined by its deviatoric and volumetric parts:

$$U = U_{dev} + U_{vol} \quad \text{(Eq. 4)}$$

The model utilizes the modified strain energy density function:

$$U\left(\underline{\gamma_i}, \eta\right) = \eta U_{dev}\left(\underline{\gamma_i}\right) + \Phi(\eta) + U_{vol}(J^{el}) \quad \text{(Eq. 5)}$$

$$U_{dev} = \sum_{i+j=1}^{N} C_{ij}\left(\underline{I_1} - 3\right)^i \left(\underline{I_2} - 3\right)^j \quad \text{(Eq. 6)}$$

$$U_{vol} = \sum_{i=1}^{N} \frac{1}{D_i}(J^{el} - 1)^{2i} \quad \text{(Eq. 7)}$$

where $\underline{\gamma_i}(i = 1,2)$ represents the deviatoric principal stretches and J^{el} represents the elastic volume ratio. The damage variable can be calculated through:

$$\eta = 1 - \frac{1}{r} erf\left(\frac{U_{dev}^m - U_{dev}}{m + \beta U_{dev}^m}\right) \quad \text{(Eq. 8)}$$

where U_{dev}^m is equal to the maximum value of U_{dev}. r is the extent of damage compared to the virgin state. The larger the r value, the less damage will occur. m controls the dependence of damage on deformation, where smaller values cause more damage (Ogden & Roxburgh, 1999).

Due to Mullin's effect, viscoelasticity, poroelasticity, and viscoplasticity on highly elastic materials, after prolonged cycling of stretch and strain, tough hydrogels become weaker (Bai et al., 2017). To prevent shakedown of the polymer network over cyclic strains and stresses, an alternative hydrogel was used composed of polyacrylamide. Polyacrylamide hydrogels contains solely covalent crosslinks (Bai et al., 2017), limiting the damage caused from Mullin's effect. The double polymer network of polyacrylamide / alginate hydrogel has ionic crosslinks, which is easily damaged in fatigue movements from Mullin's effect. The ionic crosslinks cause tough hydrogels to weaken after cyclic stretches. However, normally the ostomy adhesive will not be stretched more than 2 times its length due to the limitation of the skin stretching during locomotion, but if needed, the polyacrylamide hydrogel is an option.

Supplementary Figure 2 | Commercially-available ostomy bag adhesives. Ostomy bag can be adhered on skin by various commercially-available ostomy bag adhesives such as Karaya Gum, Stomahesive, or Osto-bond Skin Bond Latex Adhesive. Karaya Gum powder by Hollister is a polysaccharide exudate from *Sterculia urens*, an ionic hydrocolloid with 37% galacturonic acid with acetyl groups (BeMiller, 2019). The hydrophilic polysaccharides bind to hydrophobic proteins, allowing for adhesion to hydrophobic areas of the skin through weak polypeptide chain associations (Atgié et al., 2019). Stomahesive by ConvaTec is a thick hydrocolloid that acts as both an adhesive and a buffer from leaks. Osto-bond Skin Bond Latex Adhesive is a solution of rubber from *Hevea brasiliensis* which could be a mixture of an ester of acrylic or methacrylic acid with C_{3-9} ethylenically unsaturated carboxylic acid.

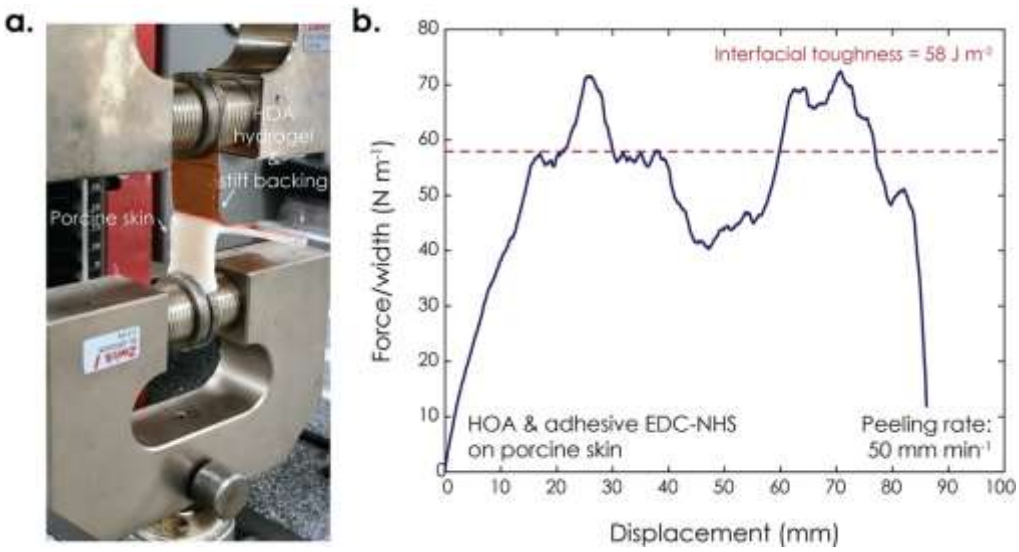

Supplementary Figure 3 | Mechanical tester setup for 180-degree peel test. a. 180-degree peel test setup based on a mechanical tester (2.5 kN load-cell, Zwick/Roell Z2.5) for HOA hydrogel adhered to a porcine skin with the chitosan tissue adhesive EDC/NHS. **b.** Representative testing curve for the 180-degree peel test at the peeling rate of 50 mm min^{-1}.

Supplementary Figure 4 | Mock ostomy setup. The setup included a plastic box with a lid drilled with a 1/4th inch hole in the center to allow plastic tubing to be thread through. The plastic tubing has a ball valve to regulate the amount of liquid flowing through the tube. The tube attaches to the 3D printed stoma part where water can flow out of the hole of the stoma.

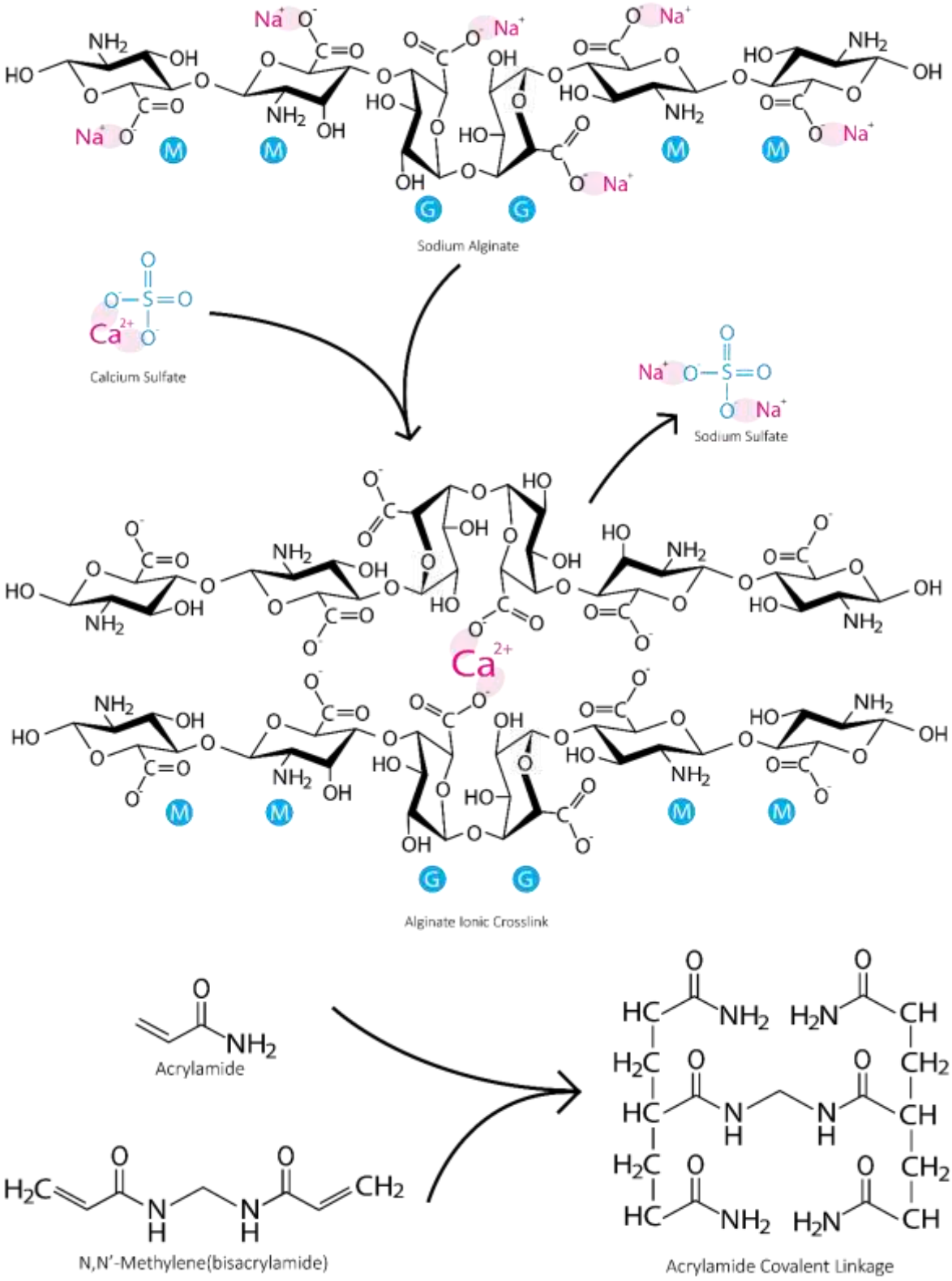
Sodium Alginate
Calcium Sulfate
Sodium Sulfate
Alginate Ionic Crosslink
Acrylamide
N,N'-Methylene(bisacrylamide)
Acrylamide Covalent Linkage

Supplementary Figure 5 | Hydrogel Polymer Formation. Sodium Alginate has a carboxylic acid group from the 6th carbon of the monosaccharide where the negative charge of the O^- ionically bonds to Na^+. Calcium sulfate ($CaSO_4$) is used for to provide Ca^{2+} ions for ionic crosslinking of sodium alginate. Acrylamide is crosslinked by *N*,*N*′-methylene(bisacrylamide) (MBAA). Interpenetrating polymer networks (IPN) of ionically-crosslinked alginate and covalently-crosslinked polyacrylamide form highly stretchable and tough hydrogel (Sun et al., 2012).

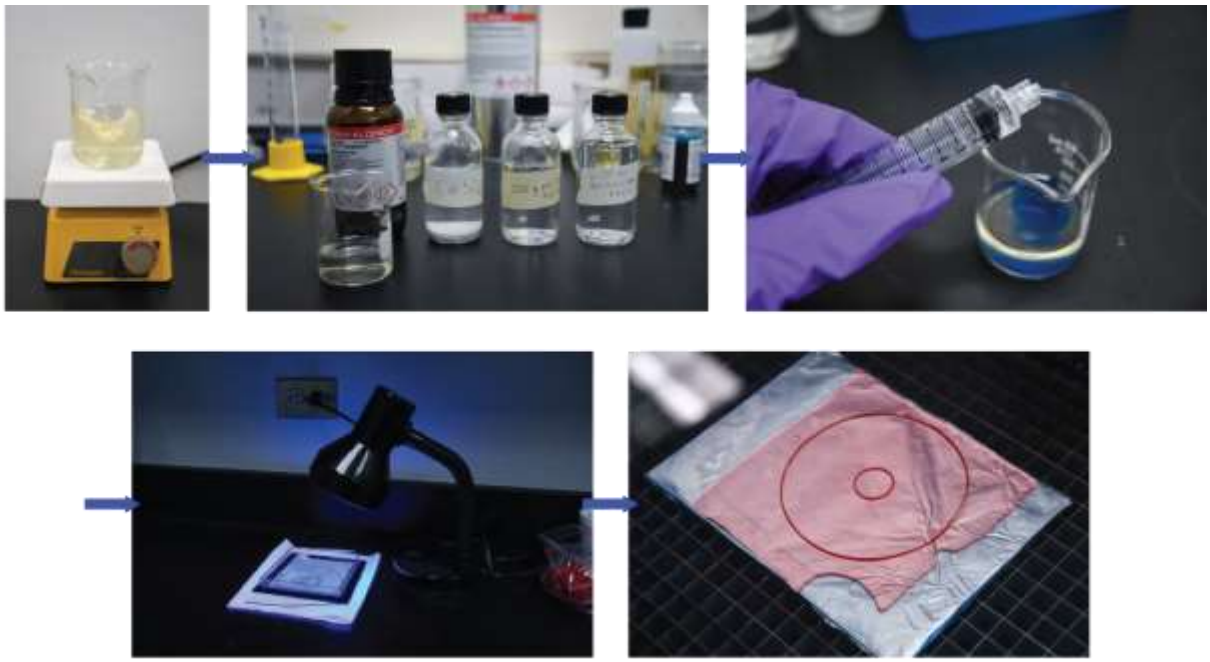

Supplementary Figure 6 | Process of making the HOA device and chitosan tissue adhesive. **a.** Acrylamide and sodium alginate monomers were dissolved in distilled water for 24 hours. **b.** MBAA, TEMED, $CaSO_4$, APS were added to the solution as covalent and ionic crosslinkers, respectively and vigorously mixed until forming homogeneous solution. **c.** Food dye was added for better visualization. Using a 10 mL syringe, the solution was passed back and forth to completely mix the solution and transfer the solution to a glass and silicone mold. **d.** The hydrogel was then cured at 365 nm UV light for 1 hour. After curing, the hydrogel was transferred onto a glass pane wrapped with aluminum foil and placed in a Ziploc bag to prevent drying. **e.** The hydrogel was then laser cut into desired shapes.

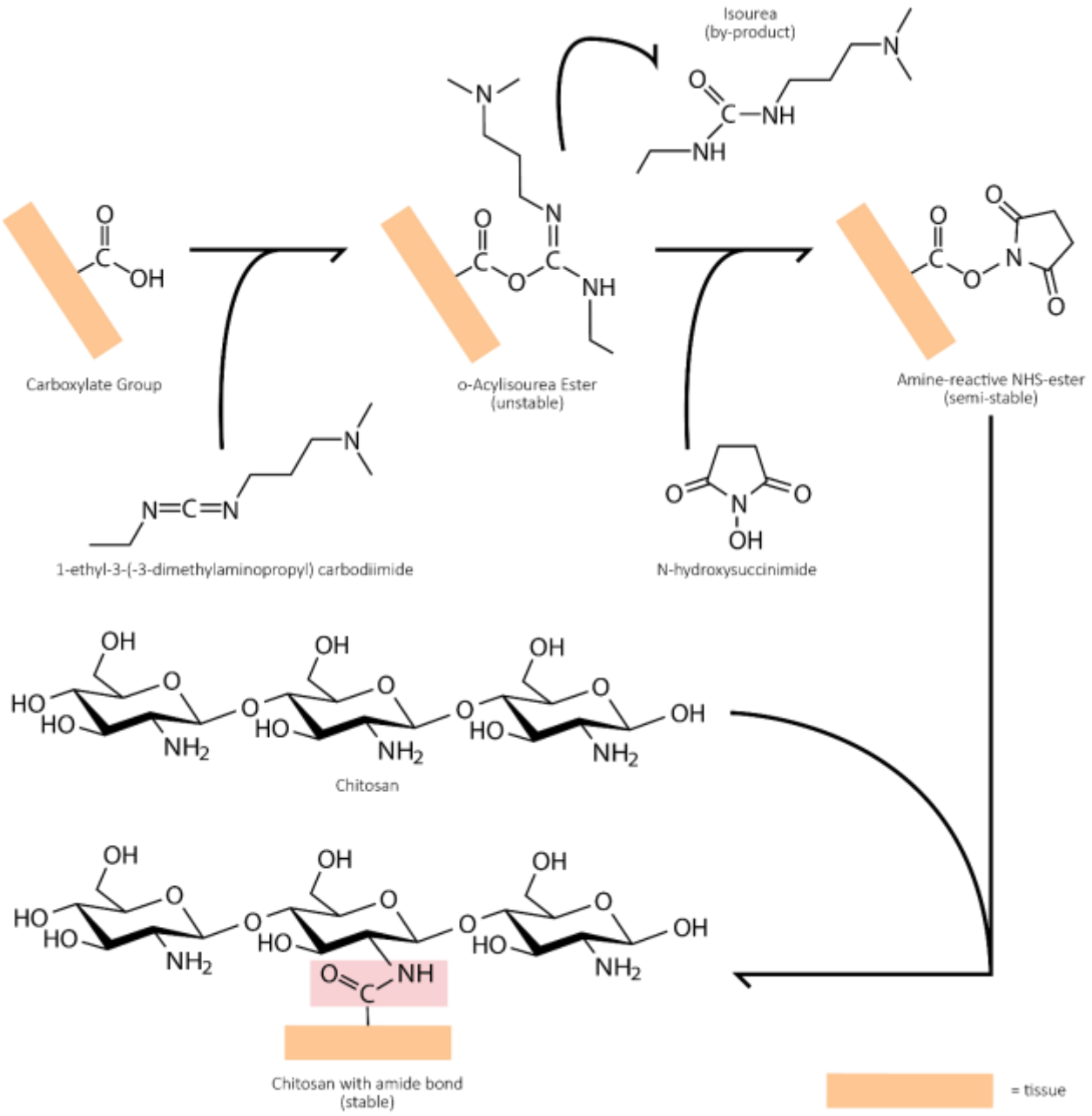

Supplementary Figure 7 | Chitosan tissue adhesive EDC-NHS bonding mechanism. Carboxylate groups in the tissue bind to 1-ethyl-3-(3-dimethylaminopropyl)carbodiimide (EDC) to form the o-Acylisourea ester. This ester is unstable that the N-hydroxysuccinimide (NHS) replaces the o-Acylisourea to create an amine reactive NHS ester, allowing for the amine group on chitosan to bond with the carboxylate group to form an amide bond.

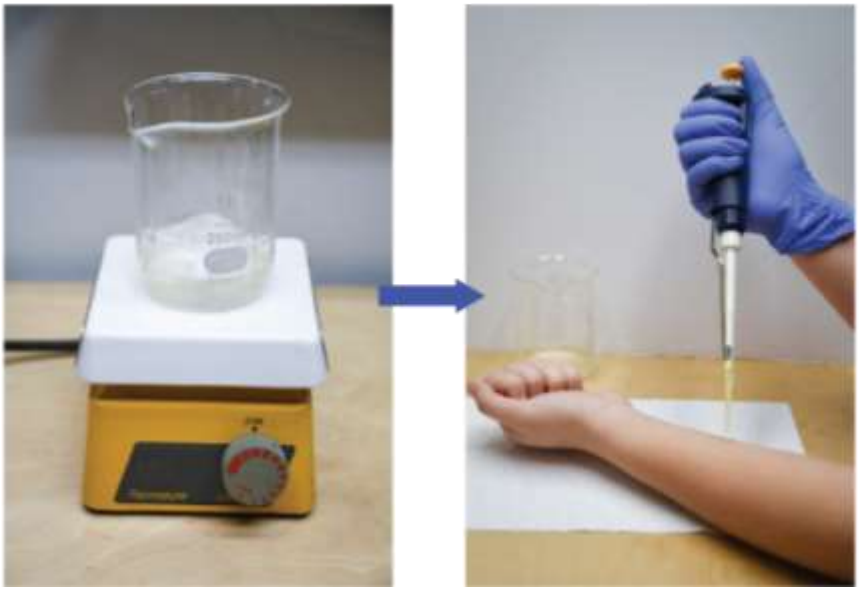

Supplementary Figure 8 | Process of making the chitosan tissue adhesive. a. Chitosan was dissolved into MES buffer (~ 6 pH). **b.** After the chitosan and MES buffer were thoroughly mixed, the solution can be applied for adhesion.

Supplementary References

Atgié, M., Garrigues, J. C., Chennevière, A., Masbernat, O., & Roger, K. (2019). Gum Arabic in solution: Composition and multi-scale structures. *Food Hydrocolloids*, *91*, 319–330. https://doi.org/10.1016/j.foodhyd.2019.01.033

Bai, R., Yang, Q., Tang, J., Morelle, X. P., Vlassak, J., & Suo, Z. (2017). Fatigue fracture of tough hydrogels. *Extreme Mechanics Letters*, *15*, 91–96. https://doi.org/10.1016/j.eml.2017.07.002

BeMiller, J. N. (2019). Gum Arabic and Other Exudate Gums. In *Carbohydrate Chemistry for Food Scientists* (pp. 313–321). Elsevier. https://doi.org/10.1016/B978-0-12-812069-9.00016-9

Ogden, R. W., & Roxburgh, D. G. (1999). A pseudo–elastic model for the Mullins effect in filled rubber. *Proceedings of the Royal Society of London. Series A: Mathematical, Physical and Engineering Sciences*, *455*(1988), 2861–2877. https://doi.org/10.1098/rspa.1999.0431

Sun, J.-Y., Zhao, X., Illeperuma, W. R. K., Chaudhuri, O., Oh, K. H., Mooney, D. J., Vlassak, J. J., & Suo, Z. (2012). Highly stretchable and tough hydrogels. *Nature*, *489*(7414), 133–136. https://doi.org/10.1038/nature11409

Zhang, T., Yuk, H., Lin, S., Parada, G. A., & Zhao, X. (2017). Tough and tunable adhesion of hydrogels: Experiments and models. *Acta Mechanica Sinica*, *33*(3), 543–554. https://doi.org/10.1007/s10409-017-0661-z